

PAP-757

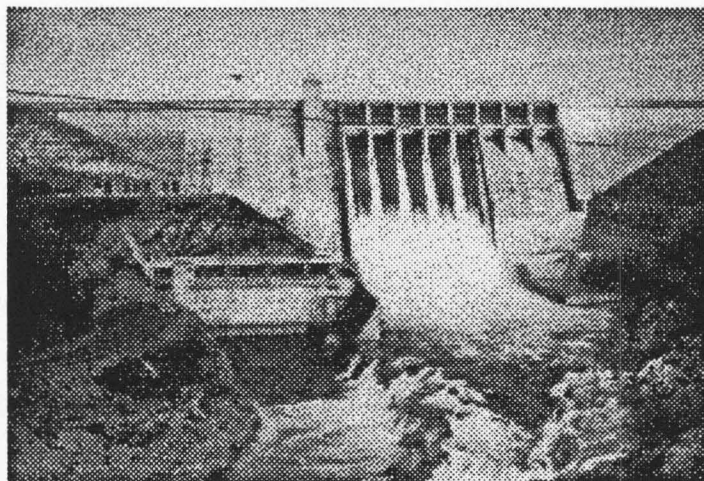
MEMORANDUM REPORT

Folsom Dam Spillway Vortices
Computational Fluid Dynamic Model Study

by

James A. Higgs

Water Resources Research Laboratory
Bureau of Reclamation



for

Mechanical Equipment Group, TSC, and
the Mid-Pacific Region, Bureau of Reclamation

February 1997

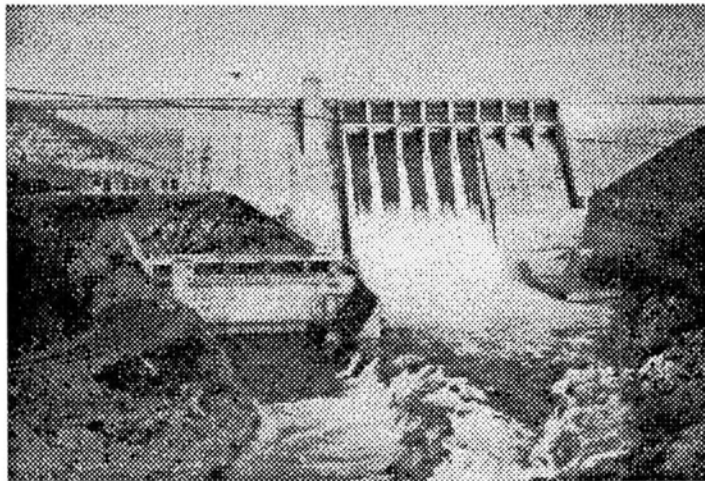
MEMORANDUM REPORT

Folsom Dam Spillway Vortices
Computational Fluid Dynamic Model Study

by

James A. Higgs

Water Resources Research Laboratory
Bureau of Reclamation



for

Mechanical Equipment Group, TSC, and
the Mid-Pacific Region, Bureau of Reclamation

February 1997

**Folsom Dam Spillway Vortices
Computational Fluid Dynamic Model Study**

By James A. Higgs

**Water Resources Research Laboratory
Water Resources Services
Denver Technical Center
Denver, Colorado**

February 1997

Acknowledgments

Thanks to Kathy Frizell from Reclamation's
Technical Service Center for providing technical
information and peer review.

This project was funded by the Mid-Pacific Region,
Bureau of Reclamation.

Front cover graphic:
Folsom Dam, California

The information contained in this report regarding
commercial products or firms may not be used for
advertising or promotional purposes and it is not to be
construed as an endorsement of any product or firm
by the Bureau of Reclamation.

CONTENTS

	Page
INTRODUCTION.....	1
Background.....	1
Scope	5
Conclusions.....	5
HYDRAULIC MODELING PREPARATION AND INVESTIGATION.....	6
CFD Program Description.....	6
Meshed Grid Development.....	6
Boundary Conditions and Model Extent	8
Obstacles and Baffles	9
HYDRAULIC MODELING RESULTS.....	10
Interpreting Graphic Results.....	10
Original Configuration.....	10
Present Configuration.....	13
Pier Nose Extension #1	16
Pier Nose Extension #2	16
Recommendation.....	16

TABLES

Table 1. Boundary conditions for the CFD models.....	8
------------------------------------------------------	---

FIGURES

Figure 1. Folsom Dam.....	1
Figure 2. Elevation view of Folsom Dam looking upstream	2
Figure 3. Crest and radial gate details	3
Figure 5. Looking downstream at the bulkhead structures	3
Figure 6. Stop log guide installation.....	4
Figure 7. Vortices observed at Folsom Dam.....	4
Figure 8. Recommended nose cone extension	5
Figure 9. Obstacle grid for the 3D model.....	6
Figure 10. Mesh and obstacles in the X-Y plane at an elevation of 428 ft	7
Figure 11. Mesh and obstacles in the X-Z plane at Y = 56.1 ft	7
Figure 12. Mesh and obstacles in the Y-Z plane at X=8.8 ft	8
Figure 13. Pressure and vectors for the original configuration	11
Figure 14. X-velocity for the original configuration.....	12
Figure 15. Cross section of the X-velocities for the original case	13
Figure 16. Pressure and vector for the present configuration.....	14
Figure 17. X-velocity for the present configuration.....	15
Figure 18. Pressure and vector for pier extension #1.....	17
Figure 19. X-velocity for pier extension #1.....	18
Figure 20. Pressure and vector for the recommend configuration.....	19
Figure 21. X-velocity for the recommend configuration.....	20
Figure 22. Cross section of the X-velocities for the recommended configuration.....	21

INTRODUCTION

Background

Folsom Dam (Figure 1) is a concrete gravity structure on the American River, and is located 20 miles northeast of Sacramento, California. Construction of the dam was by the Corps of Engineers from 1948 to 1956. Upon completion of the dam, it was transferred to the Bureau of Reclamation. It has a structural height of 340 ft. The dam crest is at elevation 481.0 ft with length of 26,670 ft, and width of 36 ft. The maximum base width is 270 ft. The total storage at water surface elevation 466 ft is 1,010,000 acre-ft.

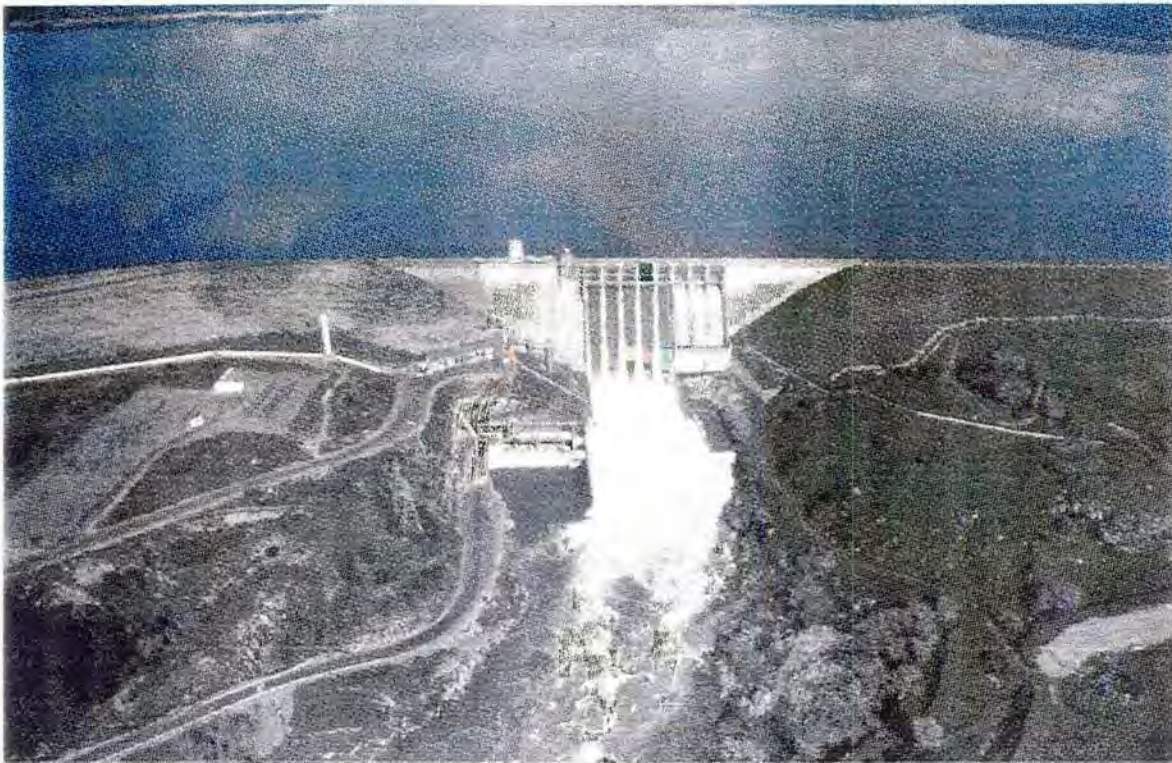


Figure 1. Folsom Dam. The five radial gates on the service (overflow) spillway are shown operating in the center of the dam. The three radial gates on the auxiliary (overflow) spillway is shown near the right side of the dam.

Folsom Dam has five 42-ft-wide by 50-ft-high radial (tainter) gates on the service (overflow) spillway (Figure 2) with the crest elevation at 418 ft (Figure 3). In addition, there are three 42-ft-wide by 53-ft-high radial gates on the auxiliary (overflow) spillway also with the crest elevation at 418 ft.

On July 17, 1995, spillway gate number three at Folsom Dam suffered a partial failure (Figure 4), which allowed an uncontrolled maximum flow of approximately 40,000 ft³/s to pass the dam. This release was well below the flow capacity of the river downstream from the dam and there was no flooding outside the levees. After the failure, a stop log guide and bulkhead arrangement were constructed upstream from the gates to allow inspection, modification, and repair of the gates (Figure 5). The guides were formed by mounting I-beams on the front of each pier (Figure 6)

Since the installation of the stop log guides and bulkhead structures, operators have reported¹ intense vortices upstream from the gates. Most of the documented released flow only had gates 2 and 5 open, and the gate 3 bulkhead in place. This caused asymmetric flows through the gates as displayed in Figure 5, which would contribute to the vortex intensity.

The report stated that on May 1, 1996, with the water surface at elevation 447.97 ft and a 3-ft-gate opening, a 4-ft-diameter vortex (measuring from the extent of the



Figure 4. Folsom gate number 3 on July 17, 1995.

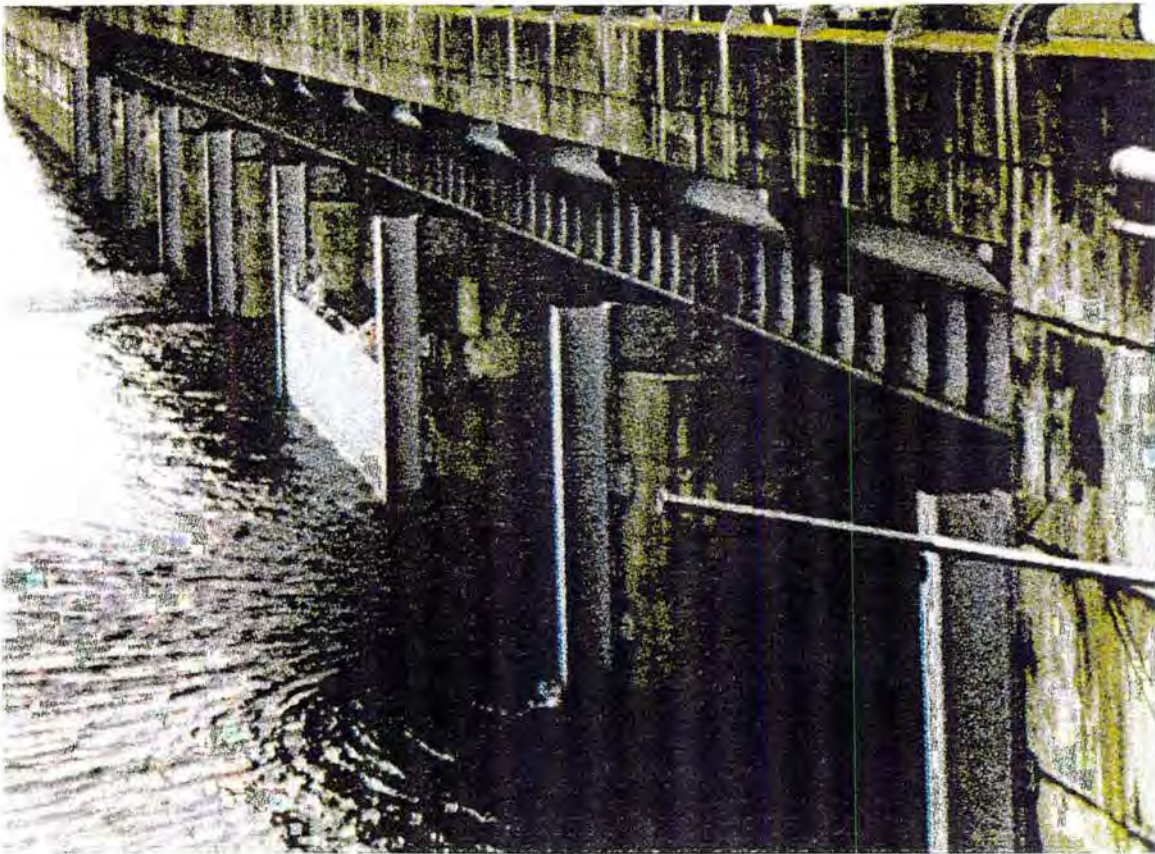


Figure 5. Looking downstream at the bulkhead structures. Newly installed I-beams can be seen on the nose of each pier. The bulkhead for spillway number 3 is in place for gate number 3 repairs. Flow lines in the water surface indicate that gates number 2 and 5 are open. The flow lines also indicate that the asymmetrical operation of the gates may increase flow separation from the pier side wall and may contribute to the vortex problem.

¹ Faxogram, Vortices Report, from Bill Joye to Chuck Howard, 7/11/96.

rotation) was observed. The vortex would appear intermittently.

On May 16, 1996 (Figure 7), gates 2 and 5 were opened to 10 ft, with the water surface at elevation 460.81 ft. The following observations were recorded

"There were vortices about 6 feet in diameter adjacent to the right and left piers about 12 feet upstream from the gate. As the vortices opened and closed, a hammering could be heard and felt. Water standing in the cross, wide flange beams of gate no. 2 was vibrating."

This describes an air core vortex, where the air core may have penetrated through the gate opening. Collapse of the air core caused the hammering effect. A penetrating air core vortex may cause spraying downstream from the gate, also called a rooster tail. This phenomenon was also observed.

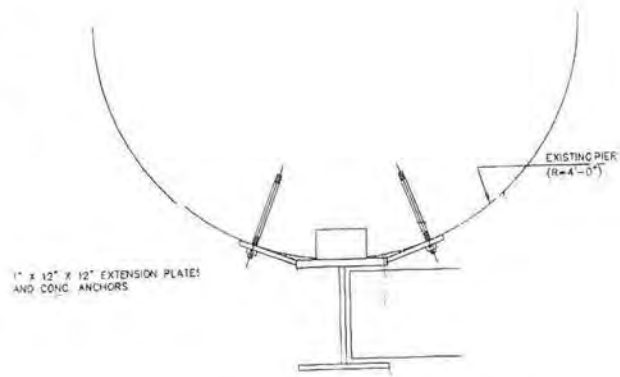


Figure 6. Stop log guide installation. The stop log guide is an I-beam that is 22 in. deep and 18 in. across.

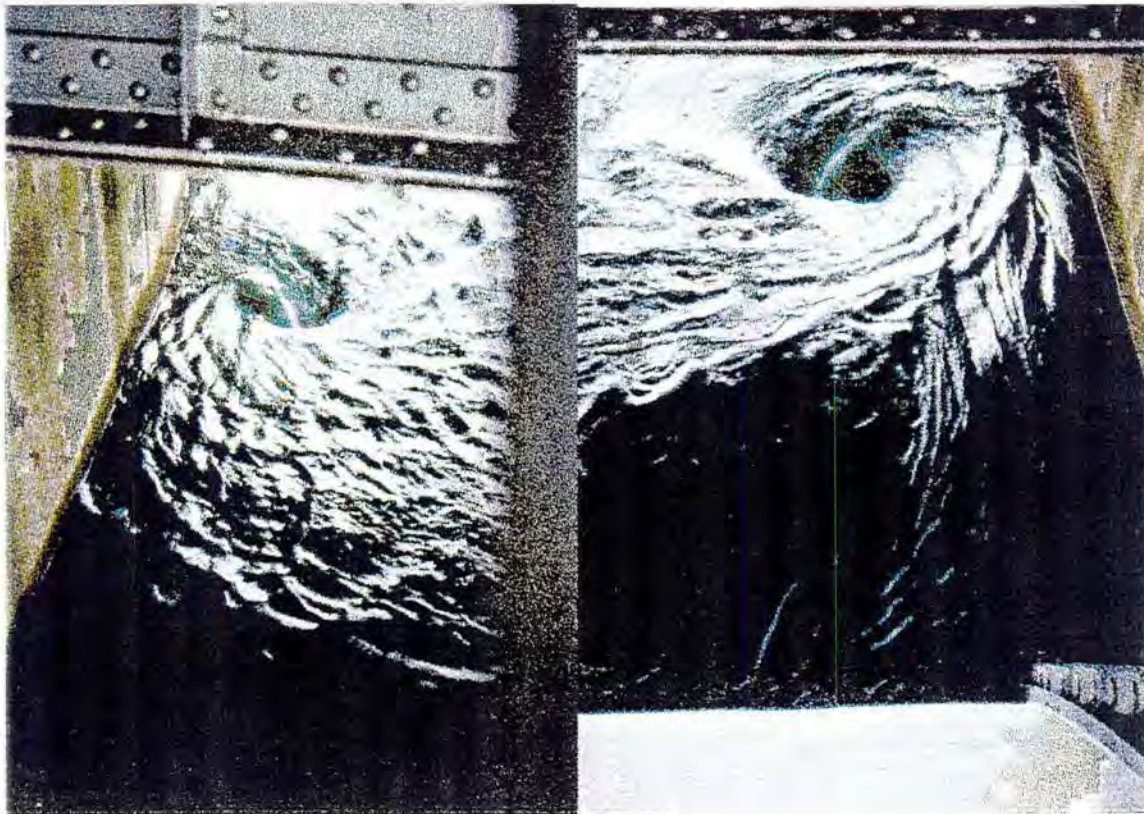


Figure 7. Vortices observed at Folsom Dam. Both of these May 16, 1996 photographs are looking upstream at the air core vortices.

The concern expressed by the operators in the report was that the newly installed stop log guides were either creating the vortices or making them stronger and more unstable which could provide additional loading on the gates leading to fatigue failure.

Scope

The objective of this study was to investigate ways of reducing vortex problems by modifying the pier nose. The study used a computational fluid dynamic (CFD) computer program to investigate the following configurations:

- The original configuration (before installation of the stop log guides) was modeled to identify the flow condition prior to the partial failure of gate No. 3.
- The present configuration was modeled with the I-beam stop log guides attached in front of the pier nose.
- Two pier nose extensions predicted to remedy the vorticity problem were modeled. The nose cone extension encased the stop log guide and will be designed to be removed when stop logs are required.

Conclusions

- Negative effects due to air core vortices will be reduced with a 3.5-ft by 8-ft elliptical nose cone as displayed in Figure 8. Vortices can not be completely eliminated for all flow conditions from any radial gate by nose cone modification.
- Identical flows through each bay will reduce the strength of the vortices.
- The flow conditions for the present configuration appears to be more unstable than for the original configuration.

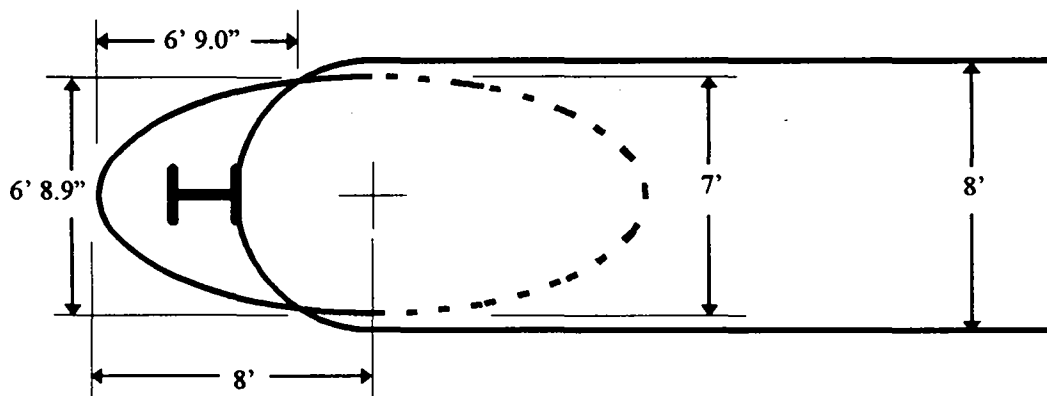


Figure 8. Recommended nose cone extension. The nose cone extension upstream from the pier and encasing the stop log guide is part of an ellipse, 7 ft by 16 ft, located at the center of the circular pier section.

HYDRAULIC MODELING PREPARATION AND INVESTIGATION

There are many steps required in developing an appropriate CFD model. These include developing, refining, and testing of the meshed grid, boundary conditions, model extents, and obstacles (structures) for the CFD program.

CFD Program Description

The CFD program FLOW-3D[®] by Flow Science Inc.², was used to model the various spillway configurations. FLOW-3D[®] is a finite difference, free surface, transient flow modeling system that was developed from the Navier-Stokes equations, using up to three spatial dimensions.

The finite difference equations are based on a fixed Eulerian mesh of non-uniform rectangular control volumes using the Fractional Area/Volume Ratios (FAVOR) method³. Free surfaces and material interfaces are defined by a fractional volume-of-fluid (VOF) function. FLOW-3D[®] uses an orthogonal coordinate system as opposed to a body-fitted system.

Final results for each model used the renormalized group theory turbulence model. This model computes the coefficients for the K-epsilon turbulence model, then solves the K-epsilon equations for each cell.

The monotonicity-preserving second order momentum approximation is a numerical option that was used to compute the velocities once the pressures for each cell were solved. It was found that this option improved flow accuracy while minimally increasing the computation time.

Meshed Grid Development

The grid meshing for the cases presented in this report were identical. The meshed grid (Figures 9-12) was designed by starting with 1-ft-long by 1-ft-wide by 1-ft-high cells in the general region of the vortex. Farther away, where less flow definition was required, the grid spacing was increased in each direction.

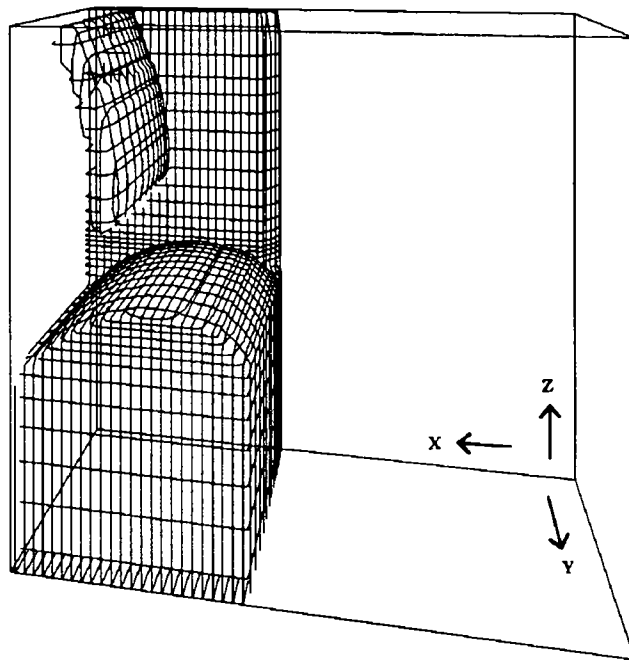


Figure 9. Obstacle grid for the 3D model. The model condition for all cases had a water surface at 447.97 ft, and a gate opening of 10 ft measured from the crest to gate bottom in the vertical direction. This view is from the back (maximum Y axis) of the model. Flow is from right to left.

² Flow Science Inc., Introduction to FLOW-3D, 1996.

³ J.M. Sicilian, "A FAVOR Based Moving Obstacle Treatment for FLOW-3D," Flow Science, Inc. Technical Note #24, April 1990 (FSI-90-TN24).

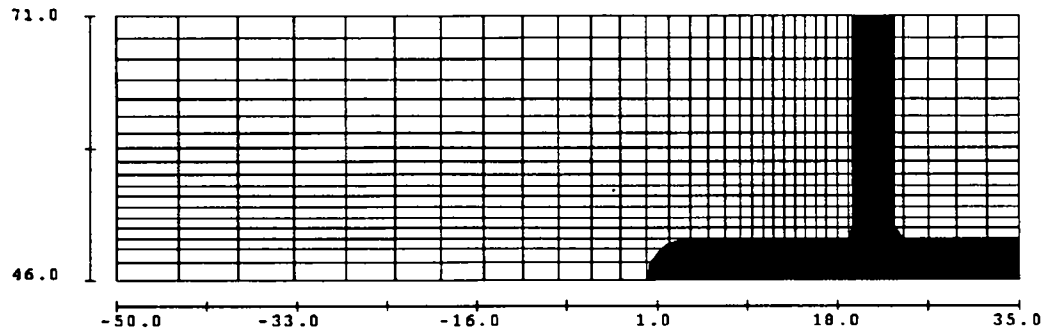


Figure 10. Mesh and obstacles in the X-Y plane at an elevation of 428 ft. A section of the radial gate can be seen in this slice. There is a 1-ft grid spacing in the X and Y direction near the pier wall, left of the gate, and downstream from the pier nose. While this graphic depicts the original configuration, all models used the same meshed grid spacing. Flow is from left to right.

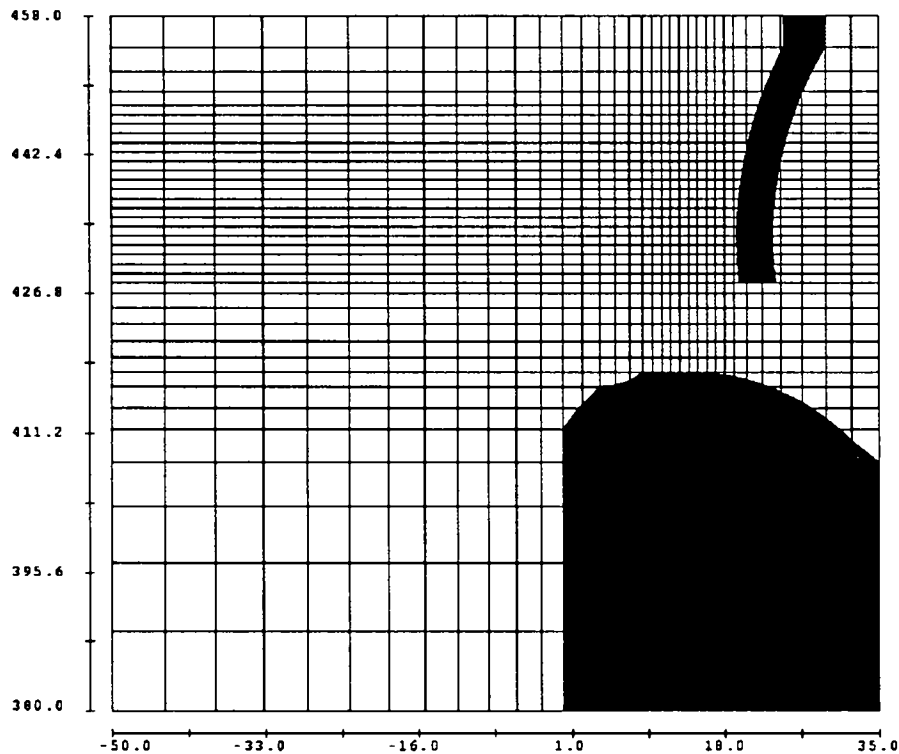


Figure 11. Mesh and obstacles in the X-Z plane at $Y = 56.1$ ft (6.1 ft from pier wall). There is a 1-ft grid spacing in the X and Z direction at the bottom of the gate from elevation 428.0 ft to elevation 448.0 ft and upstream from the gate. Coarseness of the grid in the region of the crest will effect the discharge accuracy, but should not effect vortex formation. Flow is from left to right.

While a well-defined crest shape is important for computing discharge, the crudely defined crest used in the final models had little effect on vortex formation.

Several 3D CFD models were used to determine the adequate grid spacing, model extent, computation time, and modeling performance. It was found that a grid spacing of 1 ft for the cell length in the X, Y, and Z direction in the vicinity of the vortex was optimal in view of time constraints. The 1 ft grid spacing proved adequate to detect vortex formation. However, the grid spacing was not dense enough to define the shape of the air core, but a significant surface depression forms at the center of the vortex. Typically, to model 60 seconds of prototype time on a Hewlett-Packard 9000-730 workstation required 72 hours of computation time.

Boundary Conditions and Model Extent

The flow condition selected for modeling used a water surface of 447.97 ft and 10 ft gate opening as measured from the crest. A condition with a stronger vortex was not selected due to the increased computation time involved with the larger meshed grid and higher velocities.

Boundary conditions were the same for all final models. There were six boundary conditions corresponding to the six sides of the brick-shaped meshed grid. The values are shown in Table 1.

Symmetrical boundaries have identical or "mirrored" flows on each side of the boundary.

Table 1. Boundary conditions for the CFD models.

"Brick" side	Location	Boundary condition
Left	X=-50 ft (Minimum X)	Stagnation pressure with water surface elevation 447.97 ft.
Right	X=35 ft (Maximum X)	Stagnation pressure with water surface elevation 420.0 ft.
Top	Z=459 ft (Maximum Z)	Rigid surface.
Bottom	Z=380 ft (Minimum Z)	Stagnation pressure at 4231 lbs/ft ² .
Front	Y=46 ft (Minimum Y)	Symmetrical
Back	Y=71 ft (Maximum Y)	Symmetrical

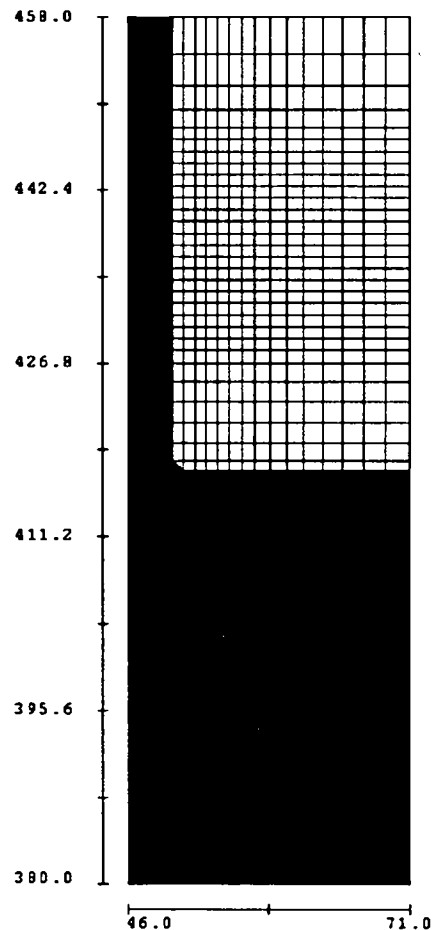


Figure 12. Mesh and obstacles in the Y-Z plane at X=8.8 ft (8.8 ft from the upstream face of the dam). The peak of the crest is not in this slice. There is a 1-ft grid spacing in the Y and Z direction between elevations 428 ft and 448 ft and next to the pier wall.

Symmetric boundaries can be used for modeling an interior spillway bay when all of the spillway gates are opened the same amount. The two X-Z boundaries, through the centerline of the pier wall (front of model) and the centerline of the spillway bay and gate (back of model), were modeled symmetrically.

Stagnation pressure boundaries are best located where the boundary plane covers a region that is nearly constant in pressure or is nearly hydrostatic. The bottom, left, and right boundaries fit this requirement if the boundary location is far enough away from the crest.

The top boundary in a free surface model can be either rigid or symmetrical. A ridge top boundary is preferable if splashing occurs.

Obstacles and Baffles

Obstacles (structures in the flow field) used by the FLOW-3D[®] solids modeler are defined by primitives (squares, cubes, blocks, planes, circles, spheres...) and quadratic functions⁴. Imported computer-aided design data can also be used by FLOW-3D[®]. This study only used primitives to define obstacles.

The obstacle definitions were the same for each model except for changes to the pier nose region. Each model included obstacle definitions for all of bay number 1 to all of bay number 7 and the face of the dam. While preliminary models used all of bay number 1 and half of bay number 2, final models only used one-half of bay number 2.

Baffles were used to define the I-beam stop log guide. Baffles, among other things, are used to block flow between adjacent cells. For the present configuration, baffles were used to block flow around the I-beam web and flanges.

⁴ Flow Science inc., Quick Reference Guide, 1995.

HYDRAULIC MODELING RESULTS

The original configuration (prior to installation of the stop log guides), the present configuration (includes the stop log guides), and two experimental pier nose extension configurations were modeled to qualitatively determine the vortex strength. Each modeled the same reservoir water surface elevation and gate opening. The reservoir water surface elevation was 447.97 ft, 29.97 ft above the spillway crest. The gate was opened 10 ft.

Each model had changing flow patterns that are characteristic of flow with vortices. Because the flow conditions were never constant, typical flow conditions are presented in the report for comparison. Quantities quoted in the results are the largest diameter vortex and highest velocities found over several time steps, and are not necessarily presented in this report.

Interpreting Graphic Results

There are two types of graphic results presented that are generated by FLOW-3D®. One is a fluid pressure and vector plot. Pressures are interpreted from the color contour bar displayed above each image. Because the pressures varied greatly from image to image, each color contour bar is unique. Fluid direction is shown by the vectors, and the length of the vector is proportional to the magnitude of the velocity. Pressures and surface depression depths discussed below are measured from the flow surrounding the vortex. Because the center surface of an air core vortex is not well defined with the mesh spacing used, the modeled surface and pressure is only indicative of vortex strength and if there is an air core.

The other graphic result is a velocity and vector plot. Velocities are interpreted from the color contour bar. To assist with interpretation between plots, velocity color contours were limited from -6 ft/s to 6 ft/s. Velocities that exceed the limits are colored the same as the limit. Large red zones have velocities that exceed 6 ft/s. Few of the dark blue zones were greater than 6 ft/s in the upstream direction. Vectors are interpreted in the same way as the fluid pressure and vector plot.

Horizontal images at elevation 434.8 ft are 6.8 ft above the bottom of the gate and show tendencies for the vortex to penetrate through the opening. Horizontal images at elevation 446.4 ft are 1.6 ft below the reservoir water surface and indicate what might be observed on the surface.

Original Configuration

The original configuration was modeled to compare changes of flow conditions with the present configuration. Results showed that vortices develop upstream from the gate that likely would have an air core that penetrates the gate opening (Figures 13-15). The surface rotation of the vortex is nearly 8 ft in diameter with a depression 1.4-ft-deep, and a maximum upstream velocity of 6.6 ft/s. Near the gate opening, a vortex is nearly 6 ft in diameter with a low pressure zone 1.6 ft deep and a maximum upstream velocity of 6 ft/s.

Comparison of successive time-plots that not displayed in this report, show that the vortex is moderately constant in strength and location.

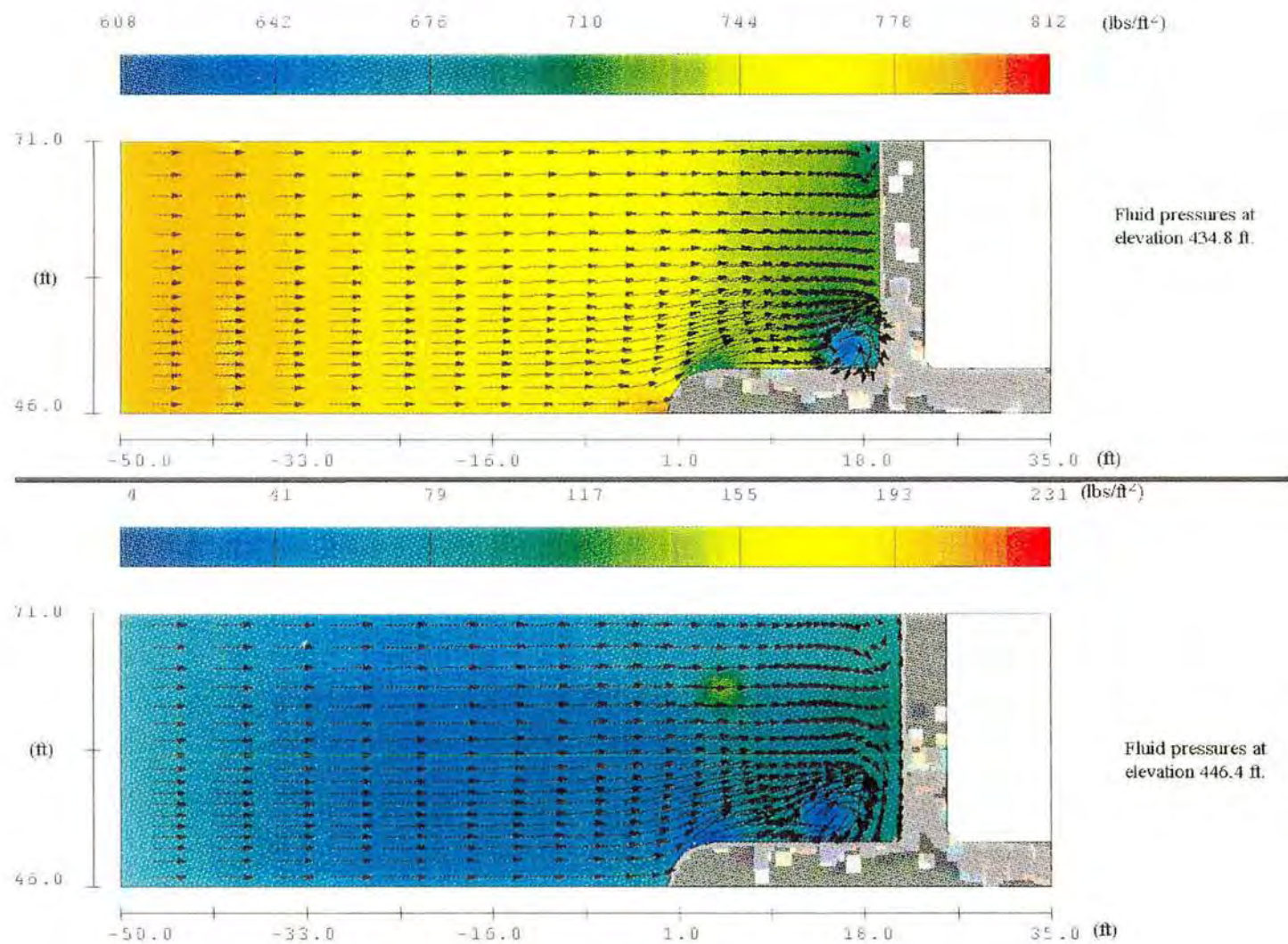


Figure 13. Pressure and vectors for the original configuration. Note that a well-defined vortex appears to penetrate through the gate opening.

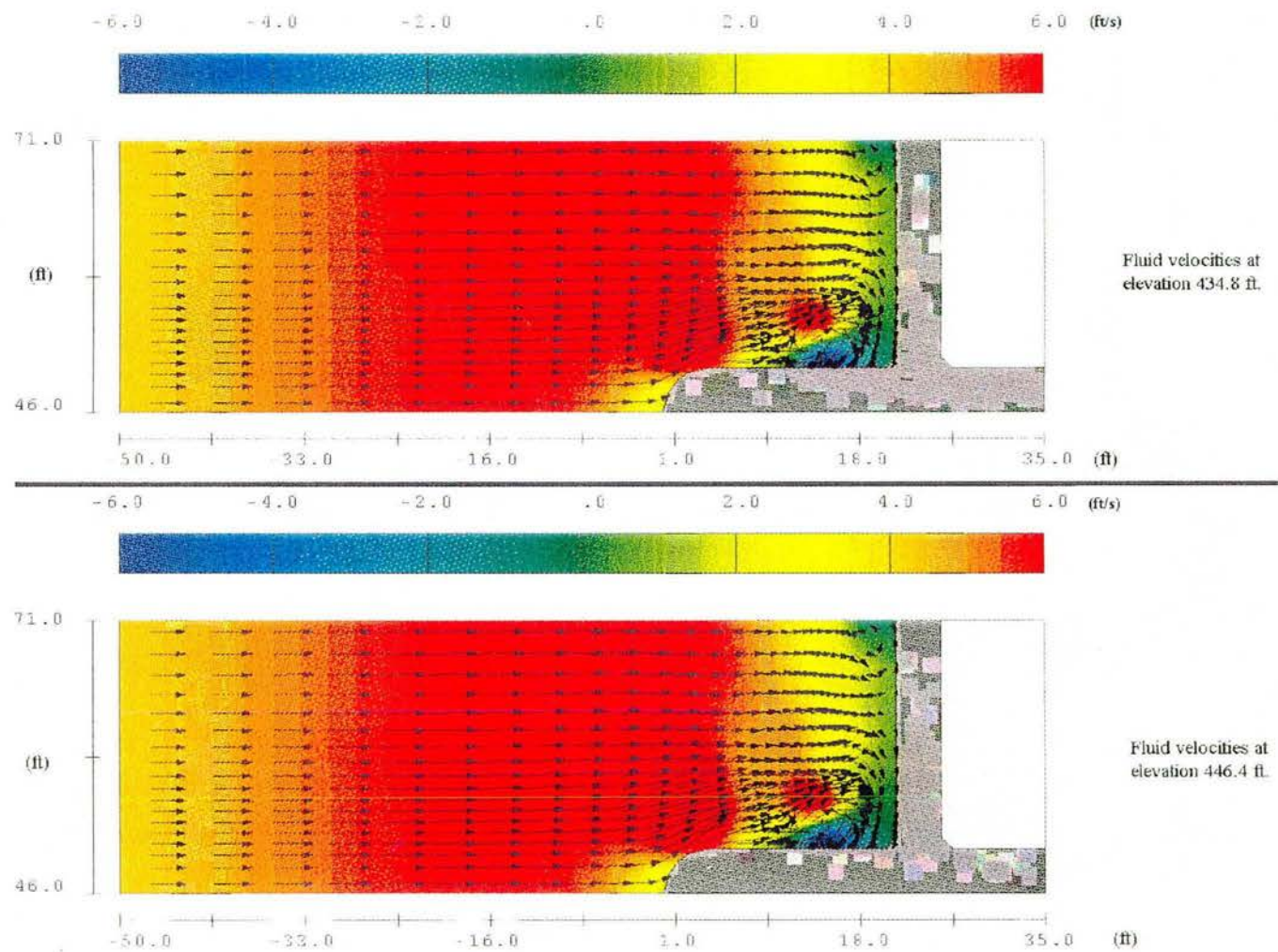


Figure 14. *X*-velocity for the original configuration.

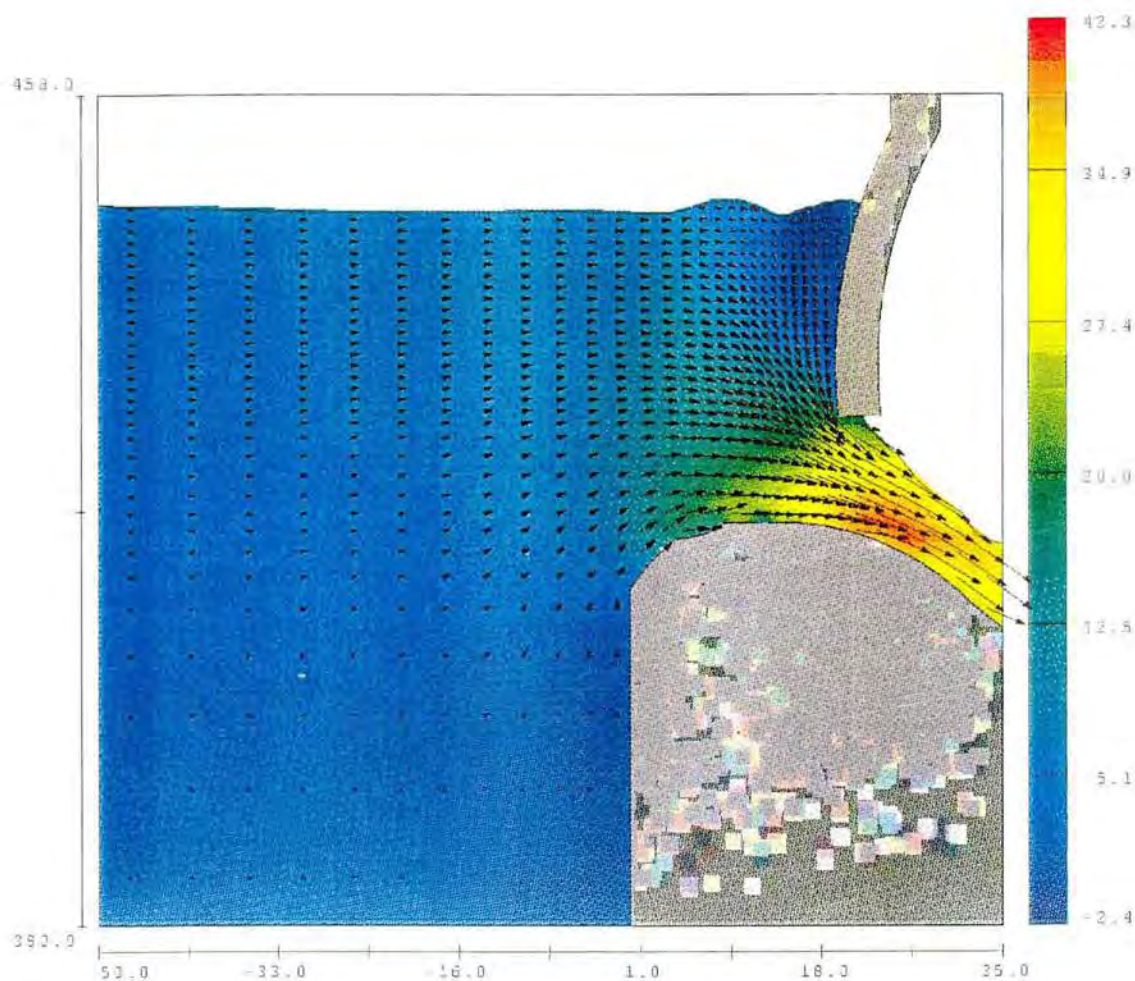


Figure 15. Cross section of the X -velocities (ft/s) for the original case. This slice was 2.5 ft from the pier side wall.

Present Configuration

The present configuration was modeled to compare the flow conditions with other models. The results are not directly comparable with the reported field conditions discussed in the background part of the introduction of this report due to the symmetrical boundary condition modeled through the pier. Model results are therefore based on near optimum gate operations. Results show that a vortex forms upstream from the gate and it likely has an air core that penetrates through the gate opening (Figures 16-17). The surface rotation of the vortex is nearly 7 ft in diameter with a pressure depression 3.2-ft-deep, and a maximum upstream velocity of 5.8 ft/s. Near the gate opening, a vortex is nearly 5 ft in diameter with a low pressure zone 1.0 ft deep, and a maximum upstream velocity of 5.1 ft/s.

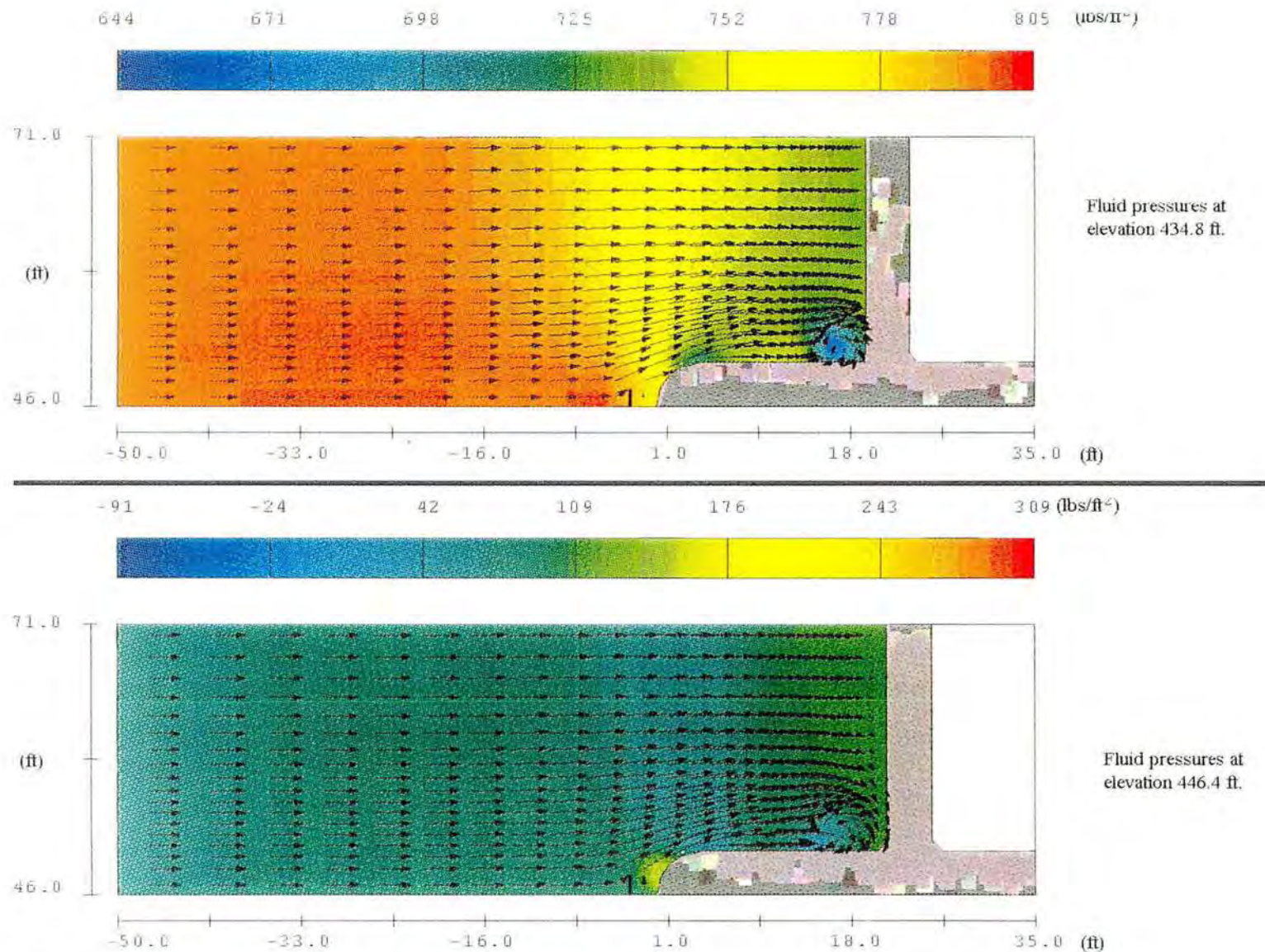


Figure 16. Pressure and vectors for the present configuration. This model displayed more fluctuations that caused adverse flow conditions than the original case. Baffles were used to block flow around the I-beam flange and web, and are displayed as a black line 1.8 ft upstream from the pier.

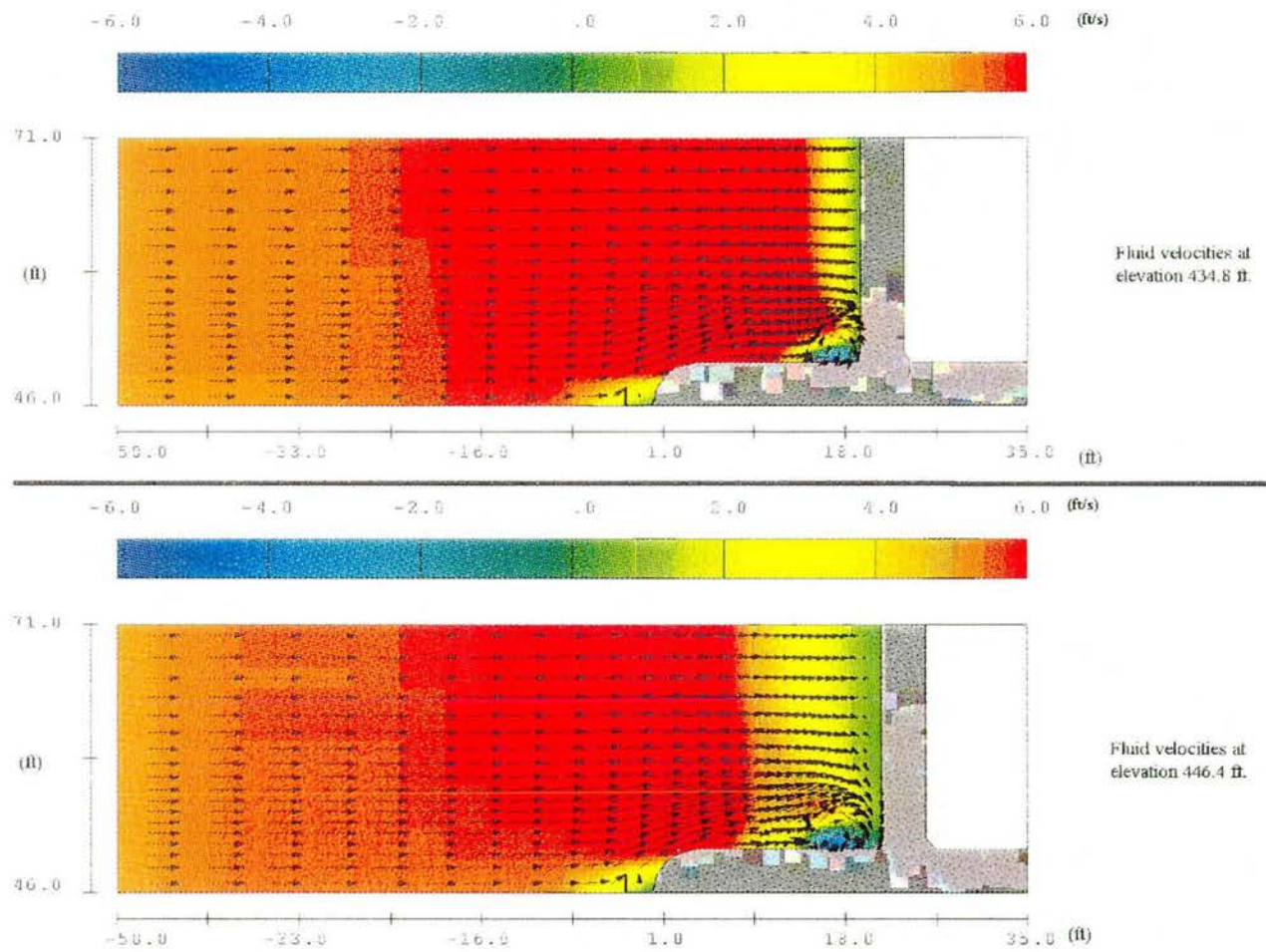


Figure 17. X-velocity for the present configuration.

This model displayed more fluctuations than the original case. Flow around the stop log guide was more turbulent and unsteady. Examination of consecutive time-plots showed the vortex to be moving and unstable. This would lead to a collapsing vortex, like the hammering effect described previously.

Pier Nose Extension #1

Pier nose extension #1 was developed from an ideal elliptical shape for flow through a non-gated spillway. The ideal elliptical shape for a pier is to have the length 3 times longer than the width. Because the piers at Folsom Dam have a width of 8 ft, the ideal length for the ellipse should be 24 ft. The center of the ellipse was modeled at the center of the existing 4-ft-radius to minimize the extension into the reservoir.

Results (Figure 18-19) show that there is a 4-ft surface flow separation from the wall and a return flow, and forms a highly distorted surface vortex. The surface depression is 1.0 ft with a maximum upstream velocity of 5.6 ft/s. Near the gate opening, the vortex is nearly 5 ft in diameter, with a low pressure zone 1.2 ft deep and a maximum upstream velocity of 4.0 ft/s.

This model displayed a slightly improved flow condition over the original and present configurations.

Pier Nose Extension #2

Because pier nose extension #1 involved a large and heavy nose pier extension, a smaller extension was investigated. Pier nose extension #2 was developed by modifying pier nose extension #1 to a smaller shape as requested by the design group. The center of the ellipse remained the same, however, the width was reduced to 3.5 ft and the length to 8 ft (Figure 8).

Results (Figures 20-22) from modeling the recommended configuration show that there is a 2-3 ft surface flow separation from the wall with minor return flow. The surface depression is 1.8 ft with a maximum upstream velocity of 2.0 ft/s. Near the gate opening, a swirl develops which is about 2 ft in diameter with a low pressure zone 0.2 ft deep, and a maximum upstream velocity less than 1.0 ft/s. The flow separation displayed may cause an intermittent vortex to form for this flow condition, but it will be much less in strength.

Recommendation

The flow condition for Pier nose extension #2 is greatly improved over the other cases and is recommended. Qualitative analysis shows that the vortex strength and instabilities can be improved with this modification.

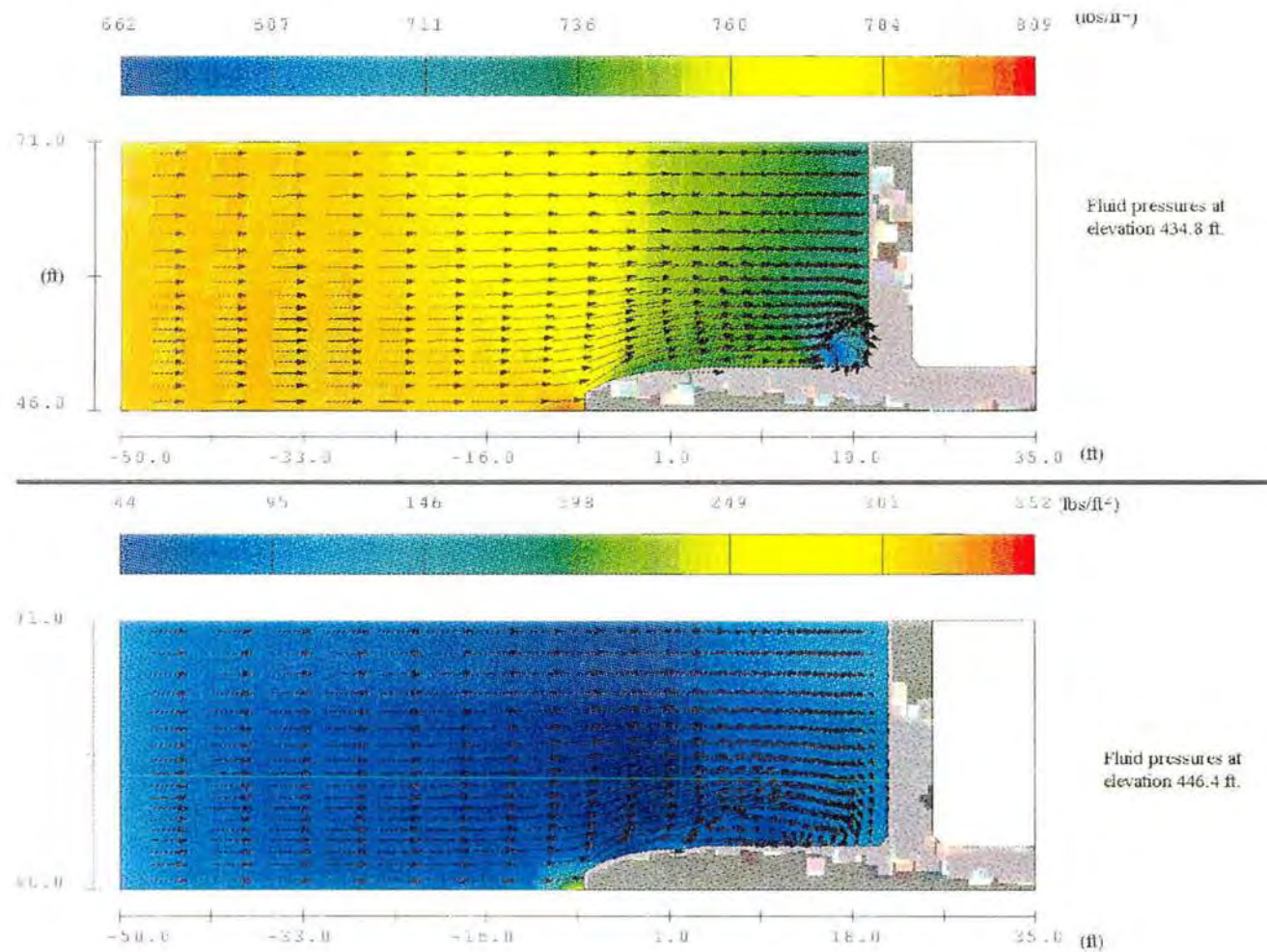


Figure 18. Pressure and vectors for pier extension #1. Flow separation can be observed near the surface. A disorganized vortex is observed near the surface. This modification displayed intermittent vortex formation.

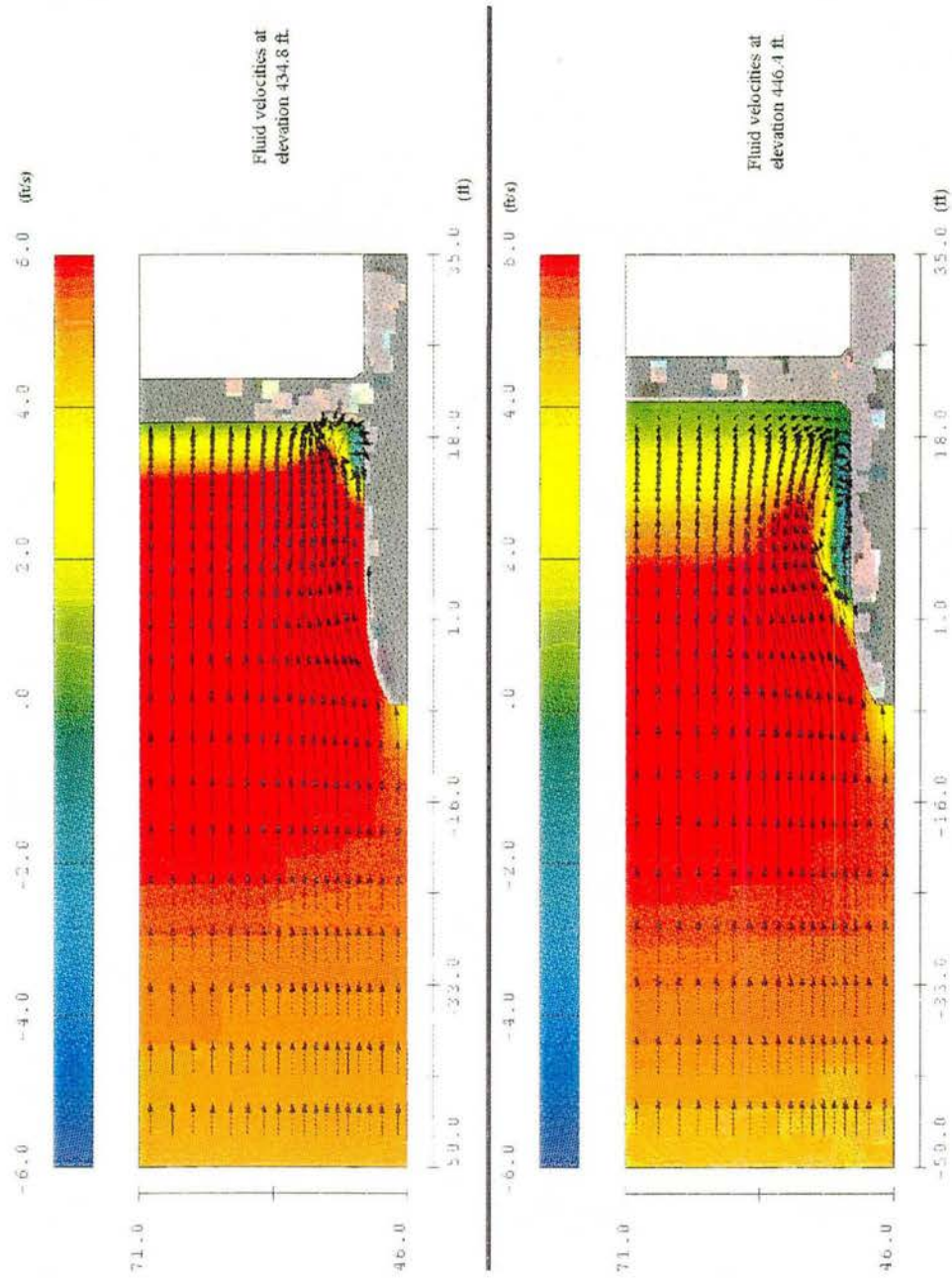


Figure 19. X-velocity for pier extension #1.

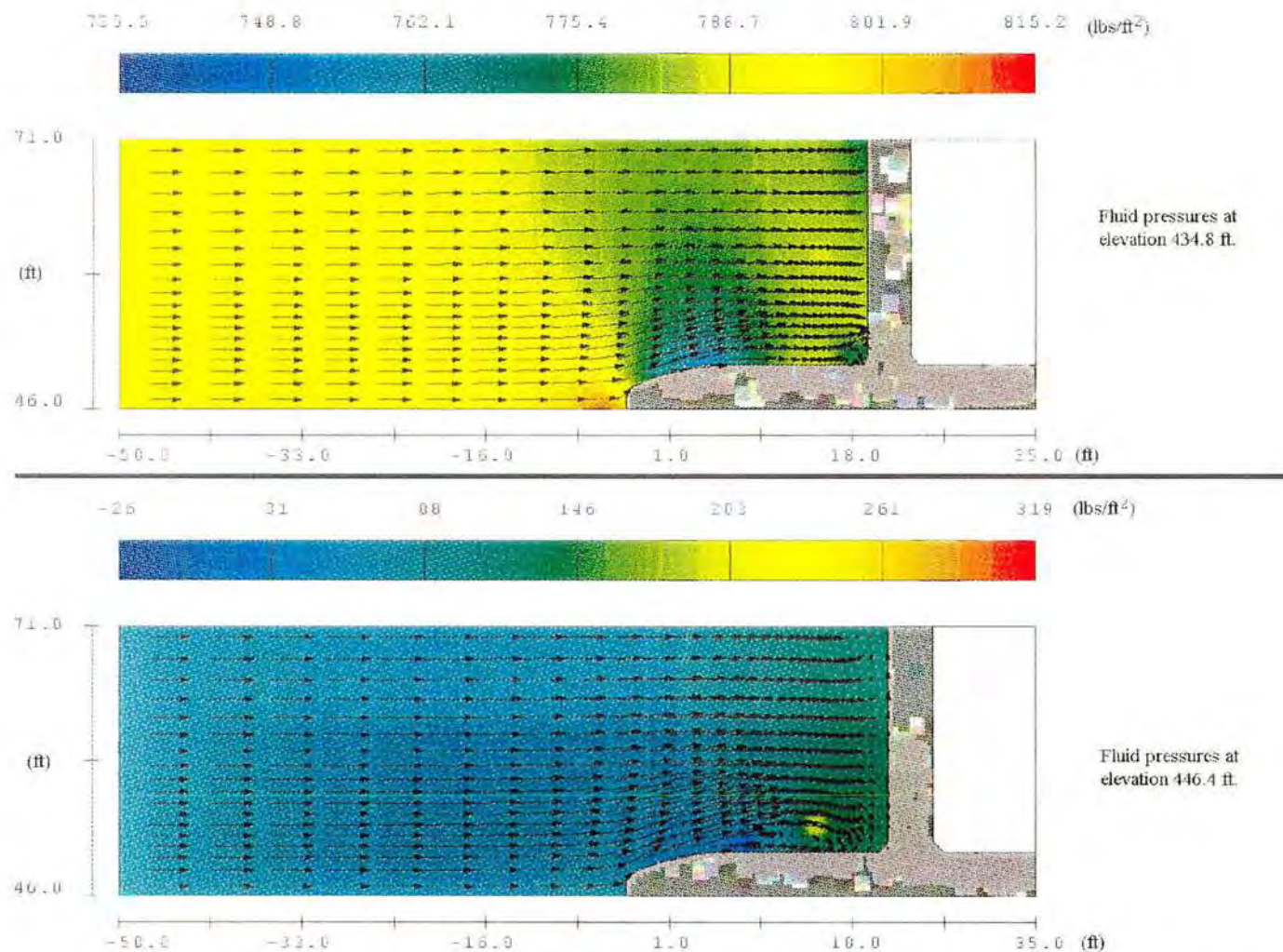


Figure 20. Pressure and vectors for the recommended configuration. Flow separation can be observed near the surface. A slight swirl is observed near the gate bottom. This modification displayed weak and intermittent vortex formation.

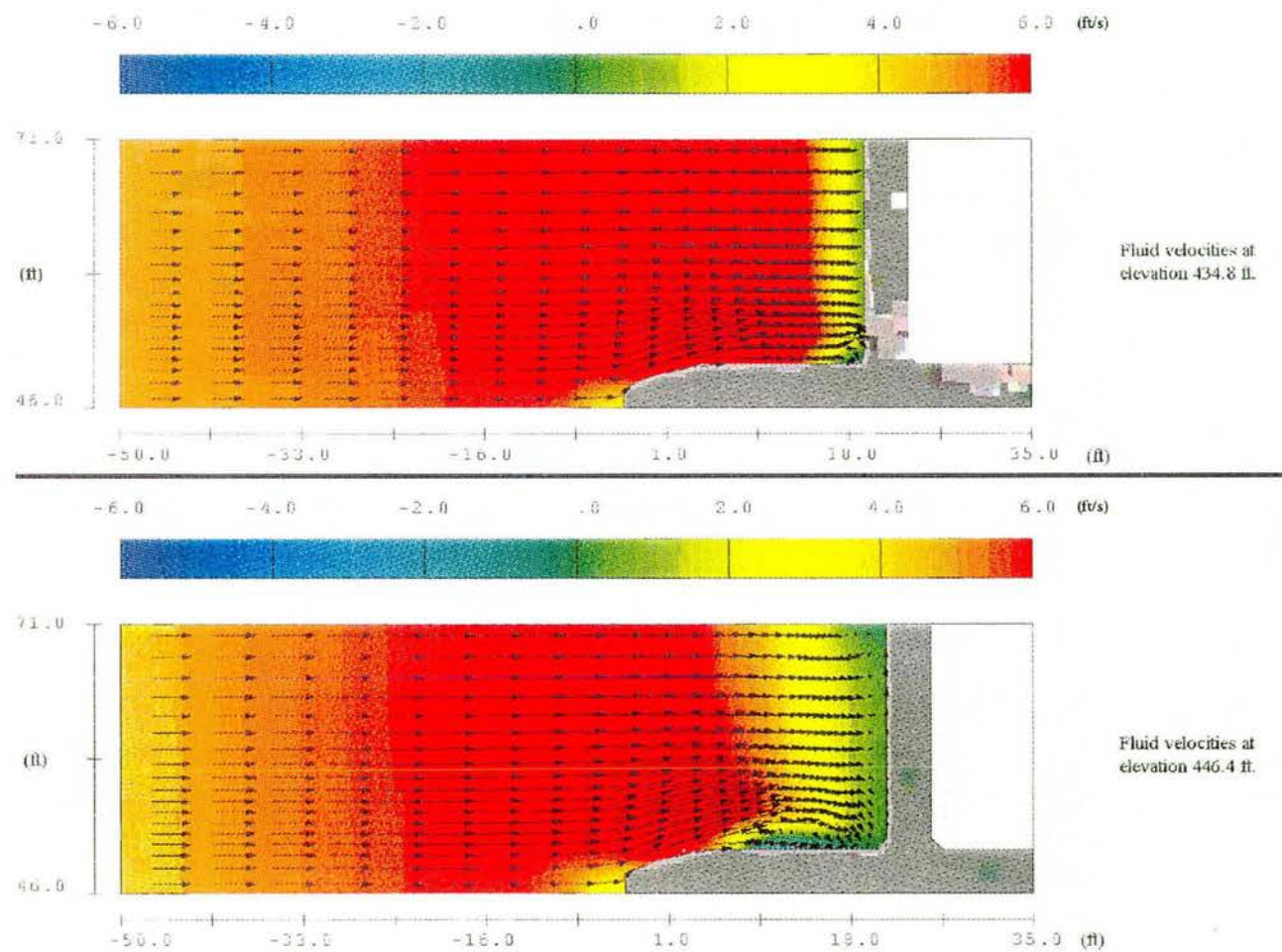


Figure 21. X-velocity for the recommended configuration.

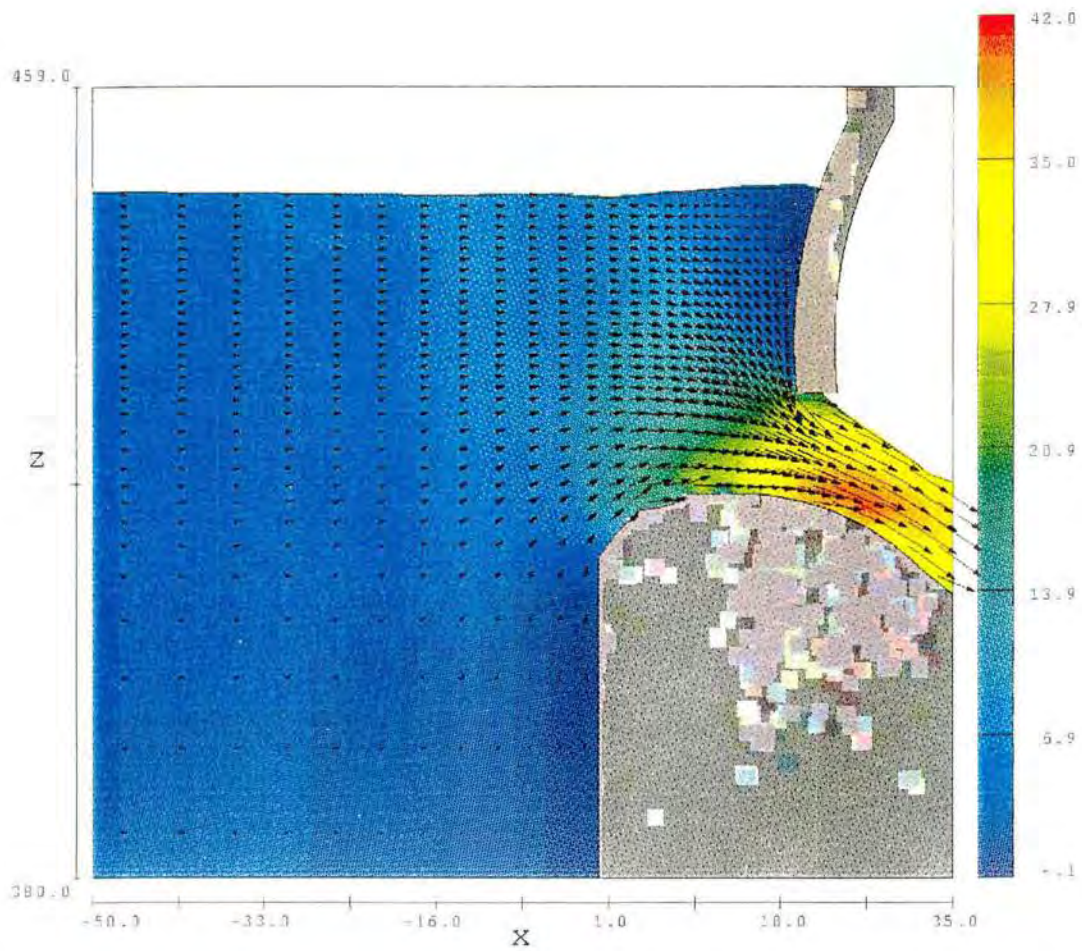


Figure 22. Cross section of the X-velocities (ft/s) for the recommended configuration. This slice was 2.5 ft from the pier side wall.